The Stripping Method for X-Ray Spectral Correction in ISO 4037-1 Narrow Spectra Series (N10-N150)

M R Nascimento[1], J C Santos [2], E M Macedo [1,3], L C P Pacífico [1,4], L A G Magalhães[4] and J G P Peixoto [1,4]

[1] Institute of Radiation Protection and Dosimetry, Rio de Janeiro, Brazil
[2] Physics Institute, Rio de Janeiro Federal University, Rio de Janeiro, Brazil
[3] Federal Institute of Education, Science and Technology of Bahia, Bahia, Brazil
[4] Radiological Sciences Department, Rio de Janeiro State University, Rio de Janeiro, Brazil

rebellomatheus99@gmail.com

Abstract. X-ray detection systems require a deep analysis of their particularities and operational limitation. In that sense, measurements with solid-state detectors can present considerable distortions due to the interaction between the photons and the detector. Therefore, to overcome these distortions, the Stripping methodology correction is extensively discussed in this paper. To evaluate the performance of this methodology, the ISO 4037-1 narrow-spectrum series from N10 to N150 was measured using a CdTe spectrometer and corrected for scape of characteristic X-ray, Compton plateau and efficiency. The corrected spectra were compared to the ISO requirements by the mean energy value and shape. It was observed that the differences between the mean energy of corrected spectra are inside the norm tolerance, except for N120 and N150, where both shape and mean energy are significantly different, with an error of 5% and 9% respectively. These results suggest that the Stripping method reduces spectral distortion being suitable for the correction of N10 to N100 radiation qualities with a CdTe spectrometer. For higher energies should be investigated other existing approaches, such as unfolding spectra techniques.

1. Introduction

The use of solid-state detectors for gamma and X-ray spectra acquisition possesses documented papers since 1966 with the NaI detector by Epp & Weis and in 1967 with the Ge detector by Drexler [1–3]. The popularity of these types of devices justifies itself since they provide a complete description of the radiation beam and, currently, for having portable options of detectors operating without cryogenic refrigeration [4–8]. X-ray spectrometry transcends the metrological applicability been also used in aerospace research for material analysis by NASA in its mission Pathfinder on Mars and Near in the asteroid Eros [9].

Nonetheless, as well as any instrumentation system, even if is well established, it is necessary to have a deep analysis of its particularities and operational limitation. In that sense, the solid-state spectrometry could not be different once spectra obtained with distinct detector materials present significative distortions, mainly those with dense and/or polyatomic sensitive volume, as the CdTe and CZT diode [6, 10–14].

Given this scenario, it will be approached a simple correction methodology that aims to reduce spectral distortion through a deep bibliographic revision presenting the Stripping model based on Di Castro [10] and Seelentag & Panzer [3] with improvements from contemporaneous approaches [11, 15]. In order to evaluate the Stripping model, this work compares the experimental radiation protection narrow spectra series (N10-150) from ISO 4037-1 of 1996 [4] based on the mean energy requirements by the norm and with the shape of PTB spectra measurements of this qualities in Ge spectrometer [16].

It is worth mentioning that those PTB spectra were published in 2000 and due to their reliability became the new standard reference of the ISO 4037-1 of 2019 [17]. It is necessary to declare that the new reference norm requires an instrument that performs invasive measurements of voltage, that is not available in the laboratory. In this case, the National Metrology Institute recommended keeping following the requirements of the 1996 version.

1.1. The challenges of a solid-state spectrometer instrumentation

Spectrometry systems require precaution in their analysis and measurements. In that sense, if we analyze a monoenergetic spectrum of photons with energy E, in an ideal situation, all photons will be detected in the same channel exhibiting an analogous shape to a Dirac delta. However, the experimental measurement presents a Gaussian distribution shape around a central value, distributing counts in other channels because of intrinsic uncertainties of the physical process and electronic characteristics of the detector [12]. Besides that, there are counts out of the Gaussian curve due to the loss of secondary photons in the diode for Compton scattering and the scape of characteristic X-ray from the sensitive volume [6, 11, 12].

In a general perspective, the physical process responsible for distorting the measured spectra in the approaching energy are mainly the characteristic X-ray scape, loss from Compton Scattering, and loss from intrinsic efficiency of the detector [3, 10]. Each one of those cited effects impacts the measured spectra according to its active volume. For instance, in this work, it is used a CdTe diode that possesses an expressive dominance of scape peaks distorting the beam in almost the whole measured energy range after 23.17 kV, because of the Cd k_α edge. On another perspective, for this diode, the Compton scattering effects are considerable over 100 keV and the detector efficiency presents more impact for energies below 10 keV and over 60 keV [6, 10, 11, 13, 18].

Therefore, the scape peaks, Compton plateau, and efficiencies issues are the target of the Stripping correction and the effects that most contribute to the spectral distortions at the study energy range. However, these are not the only challenges of this instrumentation, being only the most influential category in the ordinary use of a spectrometer recommended by the manufacturer [6, 10, 11, 15, 18–20].

1.2. The Stripping method

The idea of the Stripping method is to consider that spectra only possess photopeaks and they distribute themselves as a linear combination of Dirac's delta, equation (1). That is equivalent to saying that each photon detected produces a discrete distribution and these photopeaks can be contaminated with excess counting from X-ray scape peaks as well as a rectangular Compton plateau. In that sense, those excess counting will be removed from each channel and lastly will be corrected the efficiency of each peak [3, 10, 11, 18]. Succinctly, it is removed the photon counting that does not have their integral energy deposited in the medium and at the end of the process is given back to each channel the original lost counts due to partial energy deposition in the sensitive volume. Each stage discussed above will be detailed in the following items.

$$Counts(E) = \sum_{j}^{n} N_j \delta(E - E_j) \tag{1}$$

1.2.1. Escape of characteristic X-ray. The photoelectric interaction provides the full absorption of the photon energy, being the interaction of interest in the detection of photons [12, 21]. However, this sentence has an exception. The photon descendant from an atomic de-excitation that came from the photoelectric interaction could be able to escape from the sensitive volume producing a signal in the detector whose energy is the incident from the primary photon (E_{inc}) subtracted from the energy of the characteristic X-ray that emerged (E_{kedge}), as figure 1 illustrates. This kind of phenomena produces the so called scape peaks [6, 11, 12, 22].

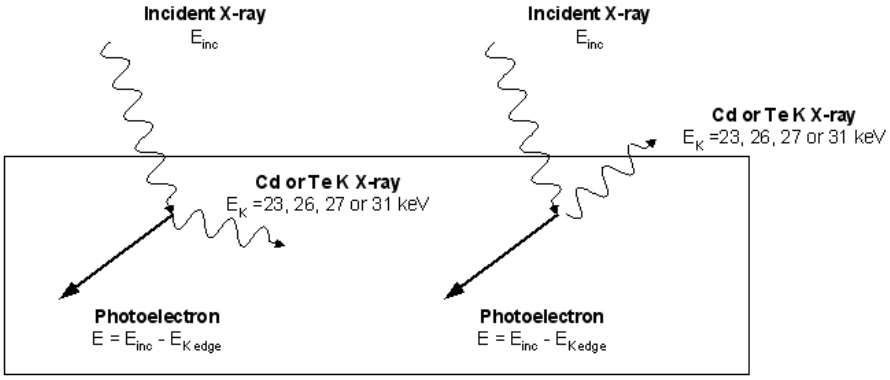

Figure 1. Scheme of X-ray escape from CdTe diode [23].

The logic behind this correction is based on firstly producing a curve that exhibits the escape probability of characteristic X-rays that are produced after N interactions (η_k) through Monte Carlo simulation [15] – alternatively, Di Castro [10] made a deterministic approach calculating the escape fraction. After that calculation, the peak scape counts, that possess energy equal to the difference between the incident photon energy and the K edge energy of detector materials ($E_{inc} - E_{kedge}$), must be removed from the *bremsstrahlung* continuum [6]. Before presenting the step-by-step of this correction, it must be understood that a generic channel of energy E_n will receive the scape counts of a photopeak whose energy is $E_n + E_k$. This idea can be clarified by analyzing carefully figure 1 and the principle of energy conservation represented by equation (2).

$$E_{inc} = E_n + E_{k\,edge} \tag{2}$$

To effectively correct this issue, it must be done the following three steps.

I. Determination of a characteristic X-ray scape fraction curve produced by photon energy, E, in the sensitive volume, $\eta_k(E)$, represented by equation (3).

$$\eta_k(E) = a + b.exp(-E/d) \tag{3}$$

Where a, b and d are constants to be adjusted.

II. Remotion of scape peak counts from channel n based on scape fraction calculated from the channel of energy $E_n + E_k$.
III. Repeat the procedure I and II for channel n-1 recursively until channel zero.

The process of removing scape counts should be performed from the higher energy channel to the zero channel for each one of the sensitive volume medium characteristics lines that are recognized to be

relevant [3, 10, 15]. Specifically for the CdTe, which is the case under analysis in this work, is considered relevant both k_α and k_β lines of Cd and Te [11, 15].

As an example, the correction procedure will analyze each channel n considering all of them scape peaks and calculate the factor $\eta_{k_\alpha}(E_n + E_{k_\alpha})_{Cd}$, $\eta_{k_\beta}\left(E_n + E_{k_\beta}\right)_{Cd}$, $\eta_{k_\alpha}(E_n + E_{k_\alpha})_{Te}$, $\eta_{k_\beta}\left(E_n + E_{k_\beta}\right)_{Te}$ multiplying then by counts on the channel of energy $E_n + E_k$. After this procedure, the fractions are subtracted from channel n, as represented by equation (4).

$$N'_n = N_n - \sum_{cl} \eta_{cl}(E_n + E_{cl}) N_{E_n + E_{cl}} \tag{4}$$

Where N_n are the counts on channel n, N'_n the new counts in the channel after suffering the escape correction and cl the acronym for characteristic lines.

1.2.2. Compton scattering correction. This correction considers Compton scattering of incident photons within the detector and the subsequent escape of the scattered photon, with energy deposition, provided only for the Compton electron [10]. This effect can occur in small detectors, such as the CdTe used in this work (1 mm thick) since the mean free path of secondary photons (of the order of several centimeters) is typically higher than the dimensions of the detector [21]. This spectral correction issue considers that each photopeak should provide a Compton plateau to the spectrum as well as the Compton continuum could be approximated to a rectangular distribution [3, 15, 18]. The last-mentioned fact is exemplified in figure 2, in which incident monoenergetic photons will deposit the full energy in the peak on the right. However, a fraction of these incident photons will interact by Compton scattering with the escape of secondary photons and energy absorption only due to the Compton electron resulting in the continuum of energies that is observed as a region with an approximately rectangular shape on the left of figure 2.

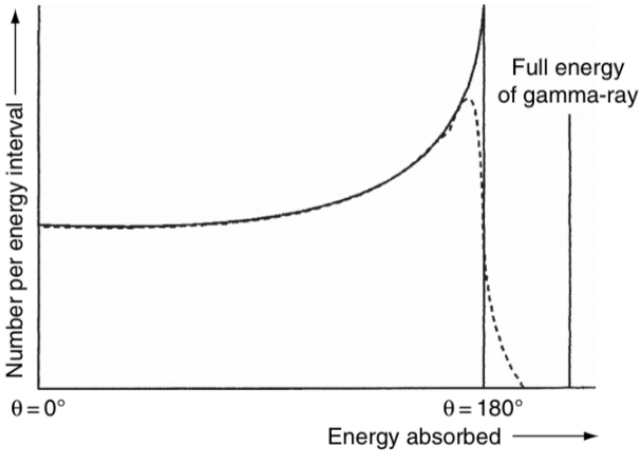

Figure 2. Compton plateau in a monoenergetic spectrum [12].

The full line in figure 2 represents a free electron scattering and the dashed line represents a coupled electron scattering [12]. In that sense, the correction of Compton events will follow five steps.

I. Determination of Compton edge energy, E_c.
II. Determination of the occurrence probability of partial energy deposition by Compton effect, η_c.
III. Determination of Compton plateau height, $h_c(E)$.

IV. Removal of counts using the plateau height, $h_c(E)$, since the Compton edge until channel zero.
V. Repeat procedure I, II. III and IV for channel n-1 recursively until channel zero.

The Compton edge energy will be given by equation (5), arising from the free-electron scattering equation of Arthur Compton in the case of maximum transference of energy, which is the backscattering [12, 15].

$$E_c = \frac{2E^2}{2E + 511} \tag{5}$$

Where E is the photon energy and 511 is the electron rest energy in keV. From another perspective, the factor η_c is given by the product of Compton effect occurrence probability in the medium multiplied by the probability of the photons not transferring their integral energy to the medium, as equation (6) represents [15, 18].

$$\eta_c(E) = \frac{\mu_c}{\mu}[1 - e^{-\mu_{en}x}] \tag{6}$$

Where μ_{en} is the absorption coefficient, μ_c the Compton attenuation coefficient, μ the total attenuation coefficient, and x is the diode depletion layer. Besides, it is worth mentioning that this work is analyzing X-ray spectra measured at the diagnostic energy range, so the absorption coefficient could also be replaced by the transmission coefficient [23]. The correction factor for this phenomenon is the mean counts of Compton events in an interval of channels. The plateau height to be removed from the spectrum for each photon of energy E is estimated using equation (7), where c is the Compton edge channel [15, 18] and $N(E)$ is the uncorrected counts in the channel energy E.

$$h_c(E) = \frac{\eta_c N(E)}{c} \tag{7}$$

1.1.1. Efficiency correction. After removing counts from the channel where they should not belong, those lost counts must be returned to their original place by the efficiency correction. This procedure will recompose the scape subtraction as well as Compton scattering and detector intrinsic efficiency loss. As discussed before in section 1.2, every channel is considered to be a photopeak and because of that consideration, the efficiency will be the photoelectric efficiency. In that context, it is calculated as the probability of occurring photoelectric interaction multiplied by the probability of the photons not being integrally attenuated in the medium. Therefore, to correct the counts in each channel, it should be divided per the efficiency, represented by equation (8) [15, 18].

$$\varepsilon(E) = \frac{\mu_p}{\mu}[1 - e^{-\mu x}] \tag{8}$$

Where μ_p is the photoelectric attenuation coefficient and μ is the total attenuation coefficient. However, one alternative approach that could be used and provides a precise and complete description of the efficiency correction is the simulation of a response function that includes the Be window of the detector as well as the electrodes and the sensitive volume without the problem of combining different attenuation coefficients to make the calculations. In that sense, when simulating a response function, it is also possible to consider charge-trapping effects and detector finite resolution [11].

2. Methodology

To evaluate the spectral correction theory discussed, it was used N10, N15, N20, N25, N30, N40, N60, N80, N100, N120, and N150 ISO 4037-1 [4] spectra qualities measured by Nascimento using an Amptek XR-100T CdTe diode detector [24]. The setup and methodology are described in previous works [6, 24]. These raw spectra were corrected using an algorithm based on the Stripping method and the results were compared to the reference ISO 4037-1 mean energy value required and to the shape of PTB spectra obtained in a Ge spectrometer [4, 16].

2.1. Correction algorithm

Based on the available literature this work implemented the spectral correction in Python programing language, as described in figure 3, which received a text file with the raw counts from the original spectrum, the energy calibration coefficients, and the X-ray tube voltage. After acquiring those data, the algorithm corrects the scape peaks, Compton plateau, and efficiency in the same order that figure 3 presents, in a channel loop ranging from the last one until channel zero and not in independent blocks of correction [3, 10]. This kind of approach is used since is noted that the distortion promoted by the scape peaks as well as the Compton plateau add counts to the low energy side of the spectra. In that context, when the loop is at the channel n, for both the effects mentioned, will be calculated factors to remove counts in the channel $n - \xi$, where ξ is a generic value, being only the efficiency correction, the factor acting in the actual channel n. Furthermore, if the correction were made in independent blocs the scape counts would be overvalued since they would encompass Compton scattering counts.

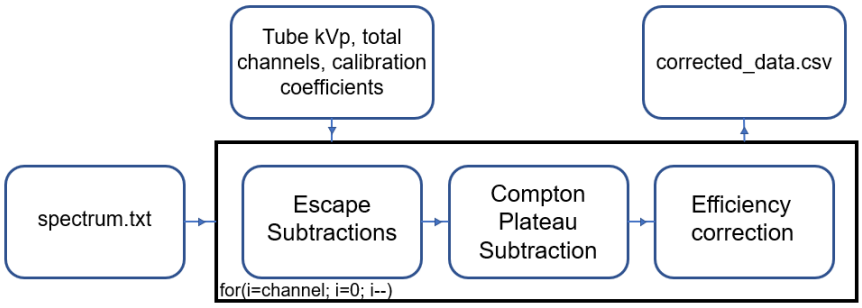

Figure 3. Flow-chart of implemented algorithm.

The proposed algorithm cuts-off the counts from channels with energy lower than 5 keV as performed by Tomal et al [11] and for 2 keV higher than the kVp value. The maximum cut-off was chosen taking into account that it is a reasonably higher value than the usual uncertainty of kVp calculations using the spectra [7, 8]. Without this consideration, the correction algorithm would certainly use pile-up data to calculate correction factors.

2.2. X-ray scape correction

When modeling the calculation of scape fractions it was used the equation obtained from Santos [15] for the k_α and k_β characteristic lines from Cd and Te. Those simulated data were fitted by an exponential equation (3) and are represented in figure 4.

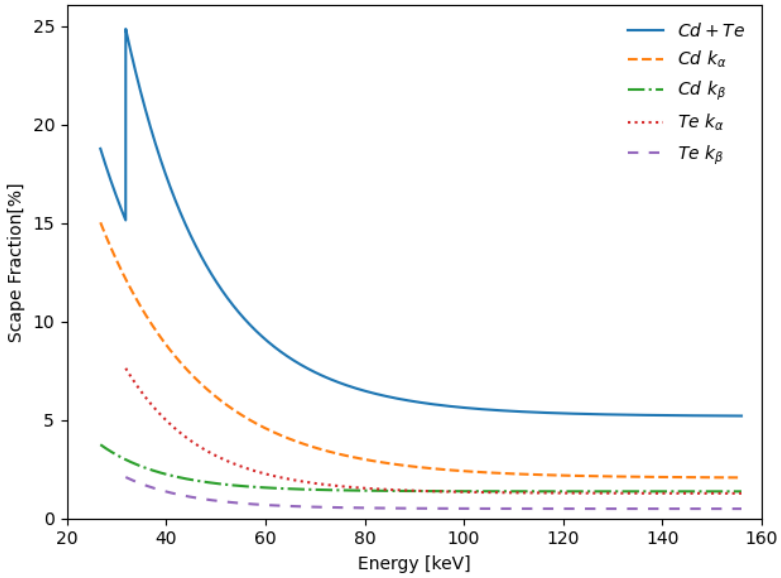

Figure 4. Scape fraction for a CdTe detector. Made using Santos equation [15].

2.3. Efficiency correction

As approached in section 1.2.3, there is a possibility of using the Terini methodology [18] or simulating a response function as Tomal et al has performed [11]. In this work, regardless of the impact that both approaches could have on the results, it was used the response function from Tomal et al. This is justified since the simulation can provide a detailed geometry taking into account attenuation provided by the Be window and the electrodes. Distinctively, when handling attenuation coefficients there is a problem of dimensionality, when combining multiple elements of attenuators, being necessary to interpolate the XCOM/NIST [25] data. The simulation is also capable of including spectral distortion effects, such as charge trapping, being an approach more physically precise [11, 26].

2.3. Quantitative parameters

The quantitative parameter was calculated based on the ISO 4037-1 definition [4]. In that sense, the mean energy is obtained by equation (8).

$$\bar{E} = \left[\sum_{i=0}^{m} N(E_i)E_i\right] \Big/ \sum_{i=0}^{m} N(E_i) \tag{8}$$

Where m is the last channel in the spectra.

3. Results and Discussion

The correction results obtained are quantitatively compared by its mean energy and qualitatively by its spectral shape in figures 5 and 6 as well as in Table 1. In the following discussion, the corrected spectra are compared to the reference values of mean energy presented by ISO 4037-1. To compare spectral shape is used the PTB spectra, that is a reference data of those radiation qualities [17].

3.1. Quantitative Analysis

The quantitative analysis of mean energy presented in figure 5 and Table 1 reveals some relevant indicators of how the proposed algorithm is working. The error bars of reference values represent the

maximum error accepted by the norm ISO 4037-1, 5% for N10-N30 and 3% for N40-N150 [4]. Each tube voltage (kV) value presented in the abscissa axis of figure 5, corresponds to an N-series spectrum quality.

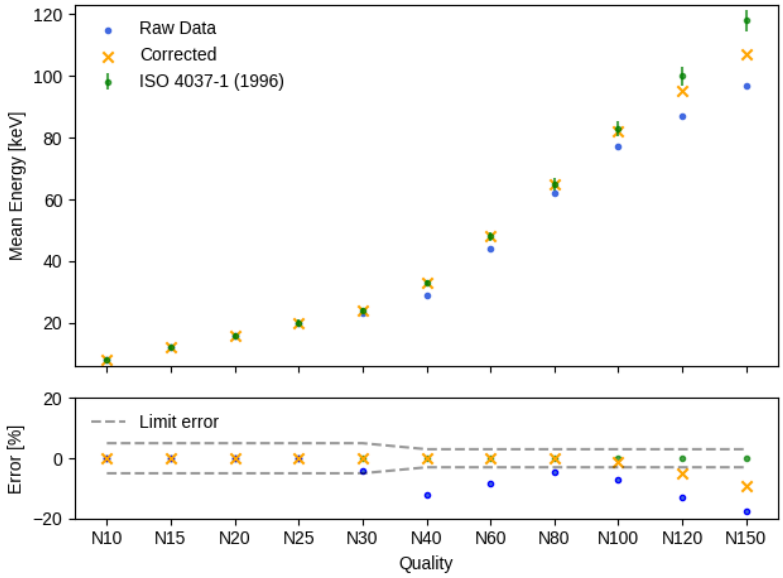

Figure 5. Mean Energy comparison.

Table 1. Mean energy (keV) comparison.

	N10	N15	N20	N25	N30	N40	N60	N80	N100	N120	N150
Raw Data	8	12	16	20	23	29*	44*	62*	77*	87*	97*
Corrected	8	12	16	20	24	33	48	65	82	95*	107*
ISO 4037-1	8	12	16	20	24	33	48	65	83	100	118

*values out of the acceptable range

The present data show that the raw spectra tend to deviate from the norm requirements as the energy of the radiation quality increase, reaching values out of the accepted range from N40 to N150 qualities, as the "*" indicates in Table 1. Actually, this is the expected behavior of this parameter as discussed in previous work since there is a significant influence of the scape peaks for most of its qualities as well as a softening of the radiation beam promoted by Compton scattering and efficiency loss for higher energies [6]. This result is one reasonable answer to the question "Why should I worry about spectral distortion effects?".

From another perspective, those spurious scenarios of beam softening are resolved for almost all the radiation qualities, except for N120 and N150 where both approaches hardened the beam when compared with the raw spectrum, but the mean energy did not match the 3% tolerance, with an error of 5% and 9%, respectively. These results suggest that the algorithm implemented in this paper corrects the spectra suitably for N10-N100.

3.2. Qualitative Analysis

Figure 6 presents the comparison between the shape of the spectra. It should be mentioned that the counts are normalized by their maximum *bremsstrahlung* value.

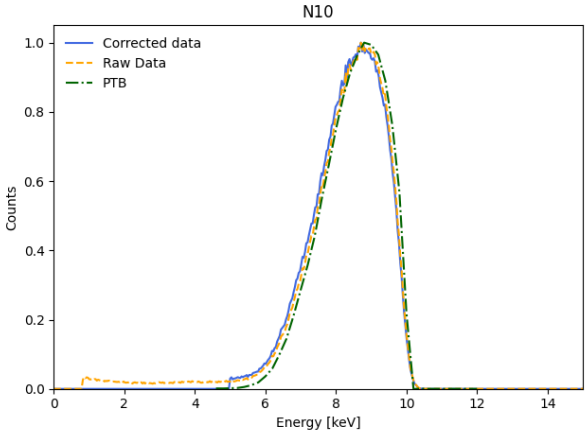
N10
Corrected data
Raw Data
PTB
Counts
Energy [keV]

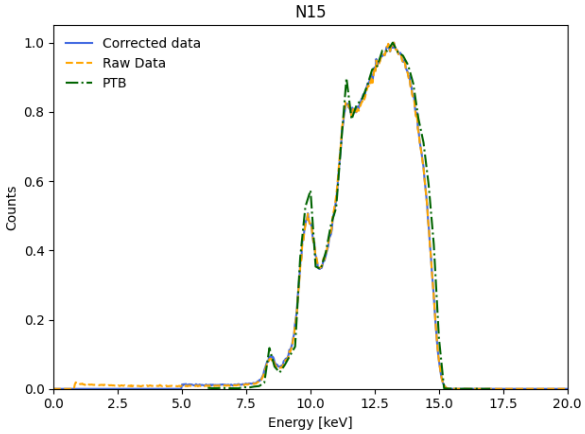
N15
Corrected data
Raw Data
PTB
Counts
Energy [keV]

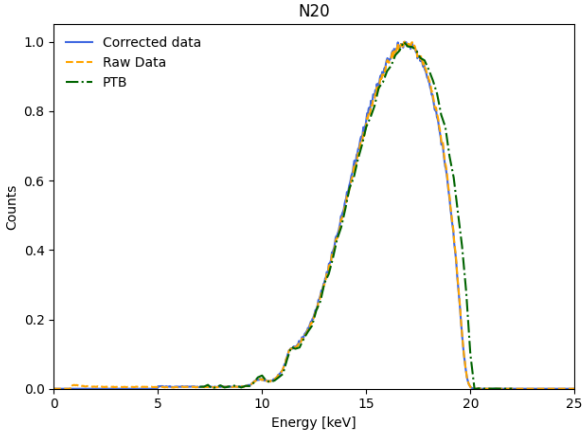
N20
Corrected data
Raw Data
PTB
Counts
Energy [keV]

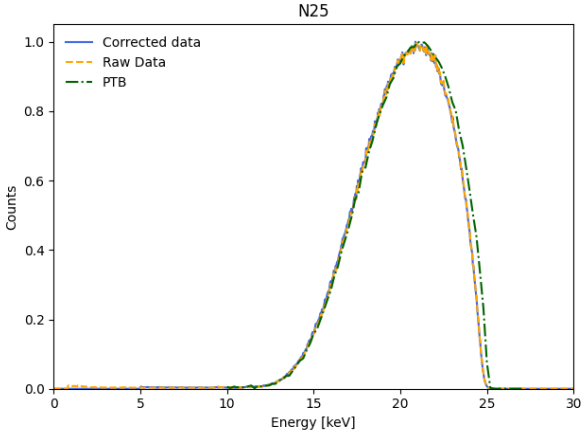
N25
Corrected data
Raw Data
PTB
Counts
Energy [keV]

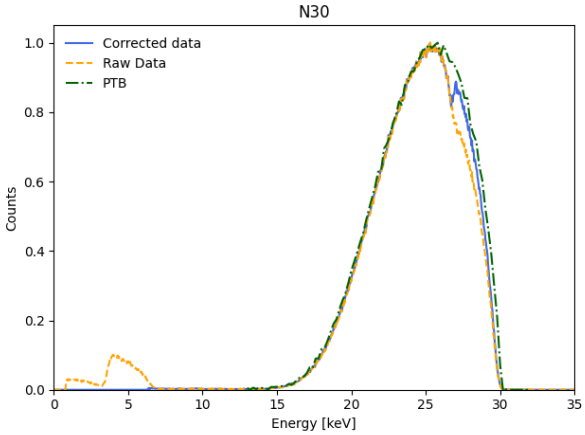
N30
Corrected data
Raw Data
PTB
Counts
Energy [keV]

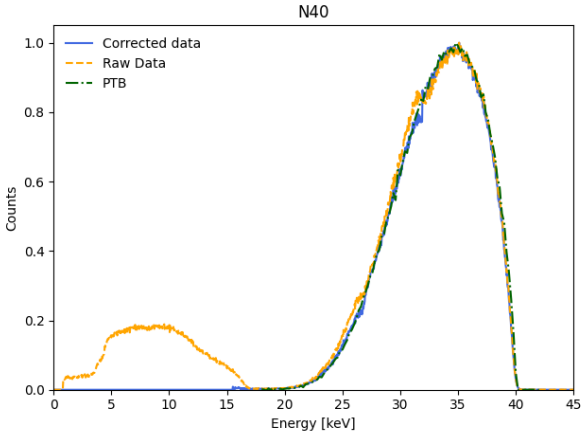
N40
Corrected data
Raw Data
PTB
Counts
Energy [keV]

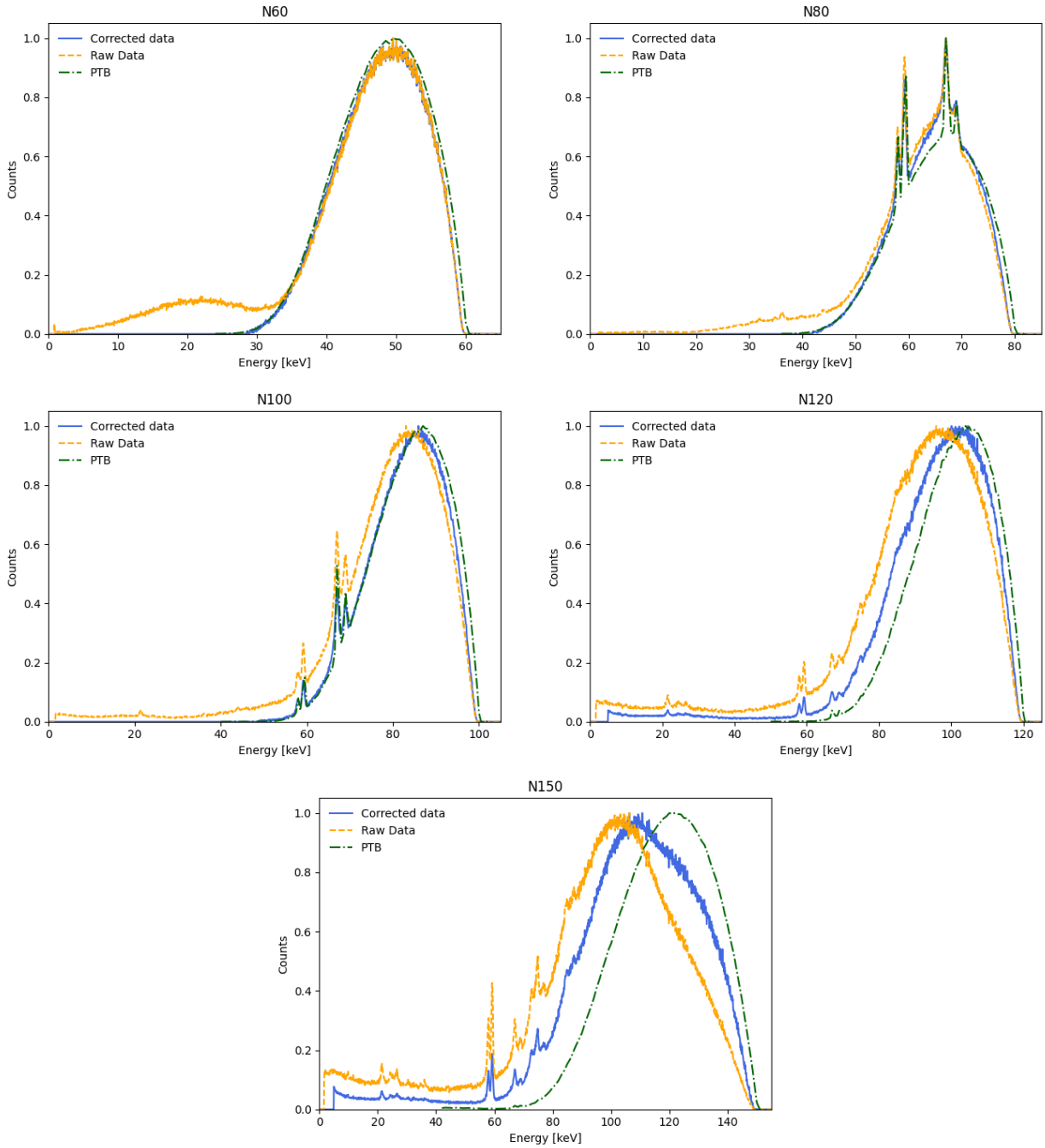

Figure 6. Qualitative shape comparison between raw, corrected and PTB spectra.

When analyzing all the spectra shapes in figure 6, it is observed that low energy spectra N10, N15, N20, and N25 presented similar shapes and intensities for all the data compared. These agreements results were under the expected behavior since there is a low Compton scattering cross-section, a high-efficiency operation of the detector under these energies, and the influence of scape events do not occur for energies below 23.17 keV, k_α from Cd, and are negligible in N25 [6]. This mutual agreement is also reinforced by Table 1 mean energy results, where the data were under the norm requirements.

For N30, N40, and N60 qualities is observed a concavity at the low energy side of the spectrum shape is completely removed by the correction algorithm. The general shape of the qualities corrected is also

similar to the PTB, except in N30 where due to the cadmium K-edge is observed a distortion near to the peak of the spectrum. This situation was not well handled by the algorithm, but the corrected one reduced the difference to the PTB. The reference spectrum does not have the K-edge situation since Ge detectors have low scape fractions [3].

According to figure 6, in N80 and N100 qualities it could be observed that the raw data do not present a concavity as mentioned before for N30, N40, and N60. For those two spectra, the beginning of a plateau formation is observed on the low energy side of the radiation quality. This is also an expected pattern, since for energies higher than 60 keV the scape fraction reduces substantially, as figure 4 suggests, and there is an increase in Compton scattering cross section, being the major distortion effect over 100 keV [10]. It should be noted that the corrected and the PTB N80 spectra present differences in intensities between the characteristic lines K_α and K_β are probably due to the worse resolution of the CdTe in comparison with the Ge spectrometer of the PTB [12].

Finally, in both qualities N120 and N150 it is possible to observe that the correction makes some changes in the shape of the raw spectra hardening the beam, as expected by the mean energy value in Table 1. However, the algorithm could not appropriately correct the quality being considerably different from the PTB standard. This result was also obtained in previous work with other measurements obtained from Pacifico's master thesis of the same qualities [27,28].

These results when analyzed with the mean energy values suggest that the algorithm could not resolve the excess of low energy counts in the left of the spectra as well as could not correct the overall shape. This issue might be expected since the Stripping presented by Di Castro and Seelentag & Panzer does not approach all the challenges of a spectrometer, correcting only three main effects that possess a significant impact on the spectra [3, 10, 11, 14, 18, 26]. Thus, this divergency above 100 kV could also be due to insufficient modeling of the Compton plateau, once it is more significant over 100 keV, as well as an effect of neglecting the charge trapping impact in the spectra [14, 26]. Besides, it should also be mentioned that this methodology considers the photopeak as a Dirac delta. However, they possess a finite resolution [26]. It is worth mentioning an interesting issue addressed by Gilmore [12] that there is a X-ray energy intrinsic uncertainty component not negligible above 100 keV for X-rays that possess a Lorentzian shape.

4. Conclusion

As discussed in this work, the X-ray spectra are a fundamental tool for characterizing radiation beams since they provide complementary information to cavities [4, 5]. For that reason, it is important not only to measure a radiation beam but also to ensure the quality of what is been measured. Therefore, correcting spectra is fundamental, and the Stripping methodology discussed is a simple approach that reduces spectral distortion, being a suitable tool for the correction of ISO 4037-1 qualities measured until 100 kV in CdTe detectors. However, above that tube voltage, the methodology starts to show some disparities when compared with the ISO standard.

After all those discussions and considerations this work brings the question if there is another physical model of spectral correction that considers the neglected physics mentioned above, that would be useful for the high energy spectra measured in CdTe. In that sense, there are authors approaching alternatives as unfolding spectra methodologies centered on the simulation of monoenergetic response functions taking into account ballistic deficit, carrier trapping, and finite resolution [14, 26, 29, 30].

5. References

[1] Drexler G, Perzl F. Spectrometry of low-energy γ- and X-rays with Ge(Li) detectors. Nucl Instruments Methods 1967; 48: 332–334.

[2] Epp E R, Weiss H. Experimental Study of the Photon Energy Spectrum of Primary Diagnostic X-Rays. Phys Med Biol 1966; 11: 302.

[3] Seelentag W, Panzer W. Stripping of X-ray bremsstrahlung spectra up to 300 kVp on a desk type computer. Phys Med Biol 1979; 24: 767–780.

[4] International Organization for Standardization. X and gamma reference radiation for calibrating dosemeters and doserate meters and for determining their response as a function of photon energy - Part 1., 1996
[5] IAEA. Technical Reports Series n0 457. Viena, 2007.
[6] Nascimento M R do, Peixoto J G P, Pacífico L de C, et al. Intrinsic challenges in x-ray spectrometry instrumentation with CdTe diode detector. Brazilian J Radiat Sci; 9. Epub ahead of print 8 August 2021. DOI: 10.15392/bjrs.v9i2C.1665.
[7] Silva M C, Herdade S B, Lammoglia P, et al. Determination of the voltage applied to x-ray tubes from the bremsstrahlung spectrum obtained with a silicon PIN photodiode. Med Phys; 27. Epub ahead of print November 2000. DOI: 10.1118/1.1318222.
[8] Terini R A, Pereira M A G, Künzel R, et al. Comprehensive analysis of the spectrometric determination of voltage applied to X-ray tubes in the radiography and mammography energy ranges using a silicon PIN photodiode. Br J Radiol; 77. Epub ahead of print May 2004. DOI: 10.1259/bjr/32514512.
[9] Amptek. Press Releases, http://www.ndtnet.com/m/amptek/press.html (accessed 30 July 2021).
[10] Castro Di, Panit R, Pellegrinit R, et al. The use of cadmium telluride detectors for the qualitative analysis of diagnostic x-ray spectra, http://iopscience.iop.org/0031-9155/29/9/008 (1984).
[11] Tomal A, Santos J C, Costa P R, et al. Monte Carlo simulation of the response functions of CdTe detectors to be applied in x-ray spectroscopy. Appl Radiat Isot; 100. Epub ahead of print June 2015. DOI: 10.1016/j.apradiso.2015.01.008.
[12] Gilmore G. Practical gamma-ray spectrometry. Wiley, 2008.
[13] Redus R H, Pantazis J A, Pantazis T J, et al. Characterization of CdTe Detectors for Quantitative X-ray Spectroscopy. IEEE Trans Nucl Sci 2009; 56: 2524–2532.
[14] Matsumoto M, Yamamoto A, Honda I, et al. Direct measurement of mammographic x-ray spectra using a CdZnTe detector. Med Phys; 27. Epub ahead of print July 2000. DOI: 10.1118/1.599015.
[15] Santos J C, Costa P R. Estudo experimental das relações entre kerma no ar e equivalente de dose ambiente para o cálculo de barreiras primárias em salas radiológicas. Universidade de São Paulo, 2013.
[16] Ankerhold, Ulrike. Catalogue of X-ray spectra and their characteristic data: ISO and DIN radiation qualities, therapy and diagnostic radiation qualities, unfiltered X-ray spectra. Physikalisch-Technische Bundesanstalt (PTB), 2000. Available by: https://doi.org/10.7795/110.20190315B
[17] International Organization for Standardization. X and gamma reference radiation for calibrating dosemeters and doserate meters and for determining their response as a function of photon energy - Part 1., 2019
[18] Terini R A, Costa P R, Furquim T A, et al. Measurements of discrete and continuous X-ray spectra with a photodiode at room temperature. 1999.
[19] Amptek. Si-PIN vs CdTe Comparison, https://www.amptek.com/internal-products/si-pin-vs-cdte-comparison (accessed 14 April 2020).
[20] Amptek. PX5 User Manual and Operating Instructions, http://atomfizika.elte.hu/muszerek/Amptek/Documentation/User Manuals/PX5 User Manual A3.pdf (accessed 14 April 2020).
[21] Knoll GF. Radiation Detection and Measurement. 4th ed. 2010.
[22] Amptek. Application Note ANCDTE1 Rev A1, https://www.amptek.com/internal-products/cdte-measurement-of-x-ray-tube-spectra-escape-events (accessed 30 July 2021).
[23] Dance D R, Christofides S, Maidment A D A, et al. Diagnostic Radiology Physics: A Handbook for Teachers and Students. 2014.
[24] Nascimento M R, Oliveira L F, Peixoto J G P. Espectrometria de raio X com detector de diodo de CdTe aplicado à metrologia. Universidade do Estado do Rio de Janeiro, 2022.
[25] NIST. XCOM/NIST, https://physics.nist.gov/PhysRefData/Xcom/html/xcom1.html (accessed 30

July 2021).
[26] Tomal A, Cunha D M, Antoniassi M, et al. Response functions of Si(Li), SDD and CdTe detectors for mammographic x-ray spectroscopy. Appl Radiat Isot; 70. Epub ahead of print July 2012. DOI: 10.1016/j.apradiso.2011.11.044.
[27] Nascimento M R, et al. The Stripping Method for X-Ray Spectral Correction at Diagnostic Energy Range. Congresso Brasileiro de Metrologia das Radiações Ionizantes, 2021.
[28] Pacífico L C, et al. Caracterização das qualidades de radioproteção N10 a N150 no laboratório de metrologia do Departamento de Ciências Radiológicas LABMETRO/DCR/IBRAG/UERJ. Universidade do Estado do Rio de Janeiro, 2020.
[29] Moralles M, Bonifácio D A B, Bottaro M, et al. Monte Carlo and least-squares methods applied in unfolding of X-ray spectra measured with cadmium telluride detectors. Nucl Instruments Methods Phys Res Sect A Accel Spectrometers, Detect Assoc Equip; 580. Epub ahead of print September 2007. DOI: 10.1016/j.nima.2007.05.147.
[30] Ankerhold, U., Behrens, R. and Ambrosi, P., X-ray spectrometry of low energy photons for determining conversion coefficients from air kerma, Ka, to personal dose equivalent, Hp(10), for radiation qualities of the ISO narrow-spectrum series, Radiat. Prot. Dosim. 81(4), 247-259, 1999

Acknowledgment
The author thanks the *Conselho Nacional de Desenvolvimento Científico e Tecnológico* (CNPq) and *Comissão Nacional de Energia Nuclear* (CNEN), for the financial support and the co-authors and IRTech research group discussions in the development of this work.